THE ASTROPHYSICAL JOURNAL, 360:577–589, 1990 September 10

THE ANOMALOUS 3.43 AND 3.53 MICRON EMISSION FEATURES TOWARD HD 97048 AND ELIAS 1: C-C VIBRATIONAL MODES OF POLYCYCLIC AROMATIC HYDROCARBONS?

W. A. SCHUTTE,[1] A. G. G. M. TIELENS,[1] L. J. ALLAMANDOLA,[1] M. COHEN,[1,2] AND D. H. WOODEN[1]

Received 1989 September 15; accepted 1990 March 9

ABSTRACT

We have obtained 5–8 μm spectra toward the two protostellar sources HD 97048 and Elias 1. Besides the well-known family of IR emission bands at 3.3, 6.2, "7.7," 8.7, and 11.3 μm, these objects show strong anomalous emission features at 3.43 and 3.53 μm. No related anomalous bands were found in the new spectra. Combining our results with earlier data, it is shown that, while the anomalous bands are emitted from within 0".05 ($\sim$10 AU) of HD 97048, the emission in the general IR features is extended on at least a 20" scale. Some possible assignments of the anomalous emission features are discussed, namely C-H stretching modes in $-$CHO or $-CH_2-/-CH_3$ groups (either in dust grains or as sidegroups on polycyclic aromatic hydrocarbon molecules [PAHs]), and vibrational modes of PAHs without sidegroups. The absence of related anomalous emissions in the 5–8 μm region as well as the high-excitation conditions in the emission zone of the anomalous features make an origin in molecular (side-)groups in grains or on PAHs unlikely. Given the high energy density in the emission zone, as well as the apparent correspondence of the anomalous 3.43 and 3.53 μm features with weak emission shoulders associated with the general family of IR emission bands, it is concluded that an explanation in terms of C-C overtones and combination bands of highly excited, large PAHs or PACs (polycyclic aromatic carbons, i.e., dehydrogenated PAHs; >500–1000 C atoms) is at the moment most attractive.

Subject headings: infrared: spectra — interstellar: grains — stars: individual (HD 97048)

I. INTRODUCTION

HD 97048, Elias 1, and HR 4049 stand alone among the objects which show the well-known family of IR emission bands near 3.3, 6.2, "7.7," 8.7, and 11.3 μm because their spectra also contain two prominent anomalous features at 3.43 and 3.53 μm (Aitken and Roche 1981; Allen *et al.* 1982; Baas *et al.* 1983; Whittet *et al.* 1983; Whittet, McFadzean, and Geballe 1984; Geballe *et al.* 1989*a*). While HR 4049 (stellar type B9.5 Ib) is believed to be a mass-losing, low-mass star, which is currently evolving into the planetary nebula phase (Geballe *et al.* 1989*a*), HD 97048 and Elias 1 are both obscured pre–main-sequence stars. As the prominent anomalous features were only recently found for HR 4049 and this object has been far less studied than the others, most of the discussion in this paper will focus on the other two sources.

Elias 1 and HD 97048 are very similar objects, classified as Herbig type A6e and B9.5e stars, respectively. Both show excess emission from dust at maximum temperatures of about 1500 K, indicating the presence of a circumstellar shell at distances on the order of a few AU with $A_v \sim 0.3$ mag (Herbig 1960; Cohen and Kuhi 1979; Thé *et al.* 1986; Elias 1978). Elias 1 seems to be variable at 2.2 μm (Elias 1978), while HD 97048 has shown no variation of the visual and near-IR broad-band photometric fluxes over an 8 yr period (Grasdalen *et al.* 1975; Glass 1979; Whittet and van Breda 1980; Whittet *et al.* 1983; Thé *et al.* 1986). Moreover, the intensities of the anomalous 3.43 and 3.53 μm bands remained constant within 10% over a 2 yr period (Aitken and Roche 1981; Whittet *et al.* 1983).

While HD 97048 shows the IR emission features in addition to the 3.43 and 3.53 μm bands, the spectrum of Elias 1 also shows the 3 μm absorption feature which is due to water ice on cool dust along the line of sight (Whittet, McFadzean, and Geballe 1984). As the spectra of HD 97048 and HR 4049 do not show any evidence for ice while the peak profiles and positions of the anomalous features are so similar to those in the spectrum of Elias 1 (Whittet, McFadzean, and Geballe 1984, see also Fig. 5 below), the interstellar ice component must be unrelated to the carrier of the 3.43 and 3.53 μm emission features. This is confirmed by speckle observations, which show that the 3.43 and 3.53 μm bands originate in close proximity to HD 97048, where the ice mantles would evaporate (Roche, Allen, and Bailey 1986).

Characterizing the carriers of the anomalous features has been particularly challenging. The band positions are suggestive of an aldehyde. Indeed, laboratory studies of formaldehyde (H_2CO) in low-temperature, interstellar ice analogs show that in such a matrix the symmetric and asymmetric C-H stretching vibrations produce IR absorption bands which are close to those observed (van der Zwet *et al.* 1985). However, in view of the speckle observations, formaldehyde frozen on ice grains can be excluded. Alternatively, an aldehyde group may be present as a sidegroup on a polycyclic aromatic hydrocarbon (PAH), the class of molecules currently thought to be responsible for the IR emission band family (Duley and Williams 1981; Léger and Puget 1984; Allamandola, Tielens, and Barker 1985). The aldehydic explanation of the anomalous 3.43 and 3.53 μm bands can be tested observationally because the IR band associated with the aldehydic carbonyl (C-O) stretch is one of the most intense IR bands known and falls between 5.75 and 6.0 μm, a region which is free from other interstellar bands. The 5–8 μm airborne observations reported here were carried out to test the aldehyde hypothesis and to search for other anomalous bands. Complementary ground based data toward Elias 1 were obtained in the 2.8–3.8 μm and the 8–12.5 μm region.

[1] Space Science Division, NASA/Ames Research Center.
[2] Radio Astronomy Laboratory, University of California, Berkeley.

In this paper it is shown that the absence of a prominent feature in the carbonyl stretching region argues against an aldehydic carrier. Other possibilities are then considered. One involves the C-H stretch in methyl ($-CH_3$) and methylene ($-CH_2-$) sidegroups on PAHs or in amorphous carbon particles. Another involves overtones and combinations of the C-C fundamental stretching vibrations (which fall in the 6–8 μm region) either in very large PAHs, PAH clusters, or large, dehydrogenated PAHs ($\gtrsim$500–1000 C atoms). It is concluded that the latter is presently the most attractive of these possibilities given the high energy density of the emission zone and the observational constraints. However, as is so often the case in interstellar PAH studies, the laboratory data needed to test this suggestion and other aspects of the PAH model are still lacking.

The paper is laid out as follows. The new observations are described in § II. This is followed in § III by a comparison of the complete spectrum of HD 97048 and Elias 1 with the normal IR emission band spectrum as well as other astronomical features. Section IV then presents a detailed discussion of the various carriers proposed, and the conclusions are drawn in § V.

II. OBSERVATIONS AND RESULTS

Spectra of Elias 1 and HD 97048 were obtained from NASA's Kuiper Airborne Observatory (KAO) between 5 and 8 μm as follows: Elias 1—1985 December 12, a single spectrum from 5.26–7.97 μm, α Tau was used as the standard star for flux calibration and to remove telluric features; 1986 August 5, two overlapping spectra were shifted by exactly one detector channel (to cover two "dead" detectors), from 5.11 to 8.01 μm and 5.24 to 8.14 μm, using β Peg as standard; HD 97048, on 1986 April 10, two overlapping spectra (shifted by exactly two detector channels) from 5.00 to 7.76 and 5.24 to 8.00 μm using α Hydra as standard star. Integration times for these five spectra were as follows: Elias 1: 12, 18, and 20 minutes, respectively; HD 97048: 18 and 24 minutes, respectively.

All 5–8 μm spectra were taken with the Faint Object Grating Spectrometer (FOGS: Witteborn and Bregman 1984) at altitudes between 12,900 and 13,600 m. Chopping of the infrared signals was at a frequency of 25 Hz with beam separations of 120″. Our aperture was always 21″ in diameter, and resolution ($\lambda/\Delta\lambda$) was $\sim$50. Wavelength calibration was achieved through repeated in-flight measurements of an internal blackbody source through a polystyrene filter. The consecutive pairs of spectra for each star were combined using $1/\sigma^2$ weighting for overlapping channels. For Elias 1 the 1985 and 1986 spectra were interlaced by treating pairs of wavelengths closer than one-half of the detector spacing as yielding a new wavelength (averaging the 1985 and 1986 wavelengths).

The spectra of Elias 1 between 2.85 and 3.79 μm and between 8.4 and 12.3 μm were obtained with the NASA/Steward 60 inch (1.5 m) telescope on Mount Lemmon, Arizona on 1987 October 12 and on October 6, respectively. For the 2.85–3.79 μm spectrum, β Tau was used as standard star. The spectrum was taken with the Short Wavelength IR Array Spectrometer (SIRAS), a liquid nitrogen–cooled grating spectrometer employing an array of 32 InSb discrete detectors. The integration time was 14 minutes. Chopping frequency of the infrared signal was 11 Hz with a beam separation of 45″. The aperture was 16″ in diameter, and the resolution was equal to ($\lambda/\Delta\lambda$) $\approx$ 100. Wavelength calibration was achieved by measuring an internal blackbody source through a calibrated standard plastic filter.

The 8.4–12.3 μm spectrum was obtained with the FOGS at a resolution of $\approx$200 using three overlapping grating settings: 8.4–10.0 μm, 9.8–11.3 μm, and 11.2–12.3 μm. Integration times were 32, 32, and 24 minutes, respectively. The chopping frequency was 11 Hz with a beam separation of 45″. The aperture was 12″, and the spectra were calibrated against α Tau. Again the wavelength calibration was obtained by measuring an internal blackbody source through a polystyrene filter and an ammonia gas cylinder.

III. THE ANOMALOUS IR SPECTRA OF HD 97048 AND ELIAS 1

a) Spectra and Spatial Distribution

The new airborne observations of Elias 1 and HD 97048 in the 5–8 μm region are shown in Figure 1. The spectra are dominated by the well-known strong 6.2 and "7.7" μm features. The "7.7" μm band peaks between 7.6–7.8 μm and 7.8–7.9 μm for HD 97048 and Elias 1, respectively. This is in the range normally found for planetary nebulae (Cohen *et al.* 1989). There may be a sharp feature at 5.35 μm in the spectrum of Elias 1 and a weak broad band at 5.7 μm for HD 97048. Broad, weak features at 5.25 and 5.7 μm have been observed toward several objects emitting the IR bands (Cohen *et al.* 1986; Cohen *et al.* 1989; Allamandola *et al.* 1989). The position, width, and relative intensity of the 5.35 μm feature in Elias 1 suggest a different origin, yet its absence from the IR spectrum of HD 97048 and HR 4049 (Cohen *et al.* 1989) implies that it is not related to the anomalous bands. Besides these bands, no new features are apparent in this spectral region. The rise toward short wavelength in the spectrum of HD 97048 is likely due to emission of circumstellar dust particles (Aitken and Roche 1981). The strong rise in the spectrum of Elias 1 starting at 8.1 μm just longward of the "7.7" μm band can possibly be explained by the onset of the intense 10 μm emission feature (Whittet *et al.* 1988; see also Fig. 3 below). No new features are apparent to a 3 σ upper limit of 7.9×10^{-18} and 7.5×10^{-18} W cm^{-2} μm^{-1}

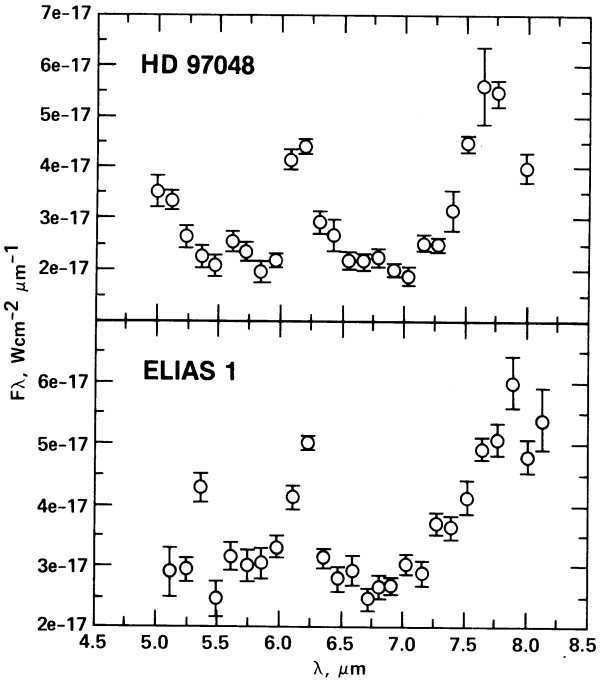

FIG. 1.—The 5–8 μm spectra of HD 97048 and Elias 1 obtained with a 21″ aperture.

for HD 97048 and Elias 1, respectively, in the 5.75–6.0 μm C-O stretching region, and to 5.6×10^{-18} W cm^{-2} μm^{-1} for both objects in the 6.8–6.9 μm $-CH_2-/-CH_3$ deformation region (see Table 2 below). Multiplying these upper limits with the expected widths of the $-HCO$ and $-CH_2-/-CH_3$ features of 0.12 and 0.13 μm, respectively (Table 2), gives upper limits of 9.5×10^{-19} and 9.0×10^{-19} W cm^{-2} for the intensities of an $-HCO$ feature towards HD 97048 and Elias 1, respectively, and 7.3×10^{-19} W cm^{-2} toward both objects for the $-CH_2-/-CH_3$ feature.

Besides the well-known 11.3 μm band, the previously published 8–13 μm spectrum of HD 97048 does not show any other emission feature (Aitken and Roche 1981). The new 8–13 μm spectrum of Elias 1 displays a silicate emission feature (Fig. 2). However, the position and shape of the feature differs from that generally observed in the interstellar medium. Figure 2 compares the band from Elias 1 to the 10 μm silicate emission feature observed toward the Trapezium stars in Orion (Gillett *et al.* 1975), to the 10 μm emission feature observed in comet Halley (Bregman *et al.* 1987) and to a band composed of the spectra of a number of interplanetary dust particles (IDPs). The Elias 1 band clearly differs from the Trapezium feature but seems to correspond rather well, including the structure at 11.1–11.2 μm, with the Halley feature and with the composite IDP silicate band. The IDPs, which provide a good fit to the Halley data (Bregman *et al.* 1987), are dominated by crystalline olivine, with smaller contributions of pyroxene and layer lattice silicates (Sandford and Walker 1985). The resolved component which falls between 11.1 and 11.2 μm in the Halley spectra and which is matched by this composite spectrum has been taken to indicate the presence of crystalline silicate material in addition to the amorphous component which is thought to be responsible for the broad, structureless feature centered near 10 μm. This structure in the Elias 1 band does not seem to correspond very well with the normal position of the 11.3 μm feature (at 11.22 μm; Witteborn *et al.* 1989) and is thus likely to originate in crystalline silicates as well. Note that there is some indication of the presence of crystalline silicates in the 8–13 μm spectra of a number of T Tauri stars (Cohen and Witteborn 1985). Higher signal-to-noise ratio data are necessary to test for the presence of crystalline silicates towards Elias 1.

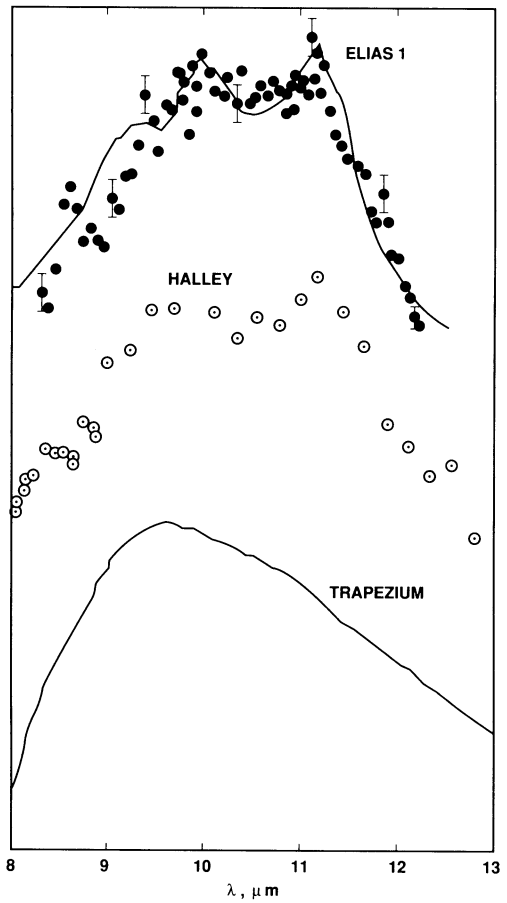

FIG. 2.—A comparison of the 8–13 μm Elias 1 spectrum of Elias 1 (*solid dots;* typical error bars are shown) with the feature emitted by the dust in the coma of comet Halley (*circles;* Bregman *et al.* 1987) and that emitted by the dust near the Trapezium stars in Orion (*lower solid line;* Gillett *et al.* 1975). The solid line superposed with the Elias 1 spectrum is an inverted absorption band produced by a composite interplanetary dust particle spectrum (*upper solid line;* Bregman *et al.* 1987).

The infrared spectral data that have been obtained on HD 97048 and Elias 1, including our new low-resolution data toward Elias 1 fron 2.85 to 3.8 μm, are summarized in Figure 3. These data were obtained using a wide range of apertures. Although taken at a smaller aperture, the 3 μm flux of Elias 1 obtained by Whittet, McFadzean, and Geballe (1984) is about 3 times higher than the flux of our data in this region. This difference may be due to the variability of Elias 1, since these data were obtained more than 3 yr apart (1984 February and 1987 October, respectively). It must be noted, however, that earlier observations obtained in 1981 November (Whittet *et al.* 1983), as well as recent data (Tokunaga 1988), have flux levels that differ no more than 30% from that of our new data.

The variations of the aperture sizes at which the spectral

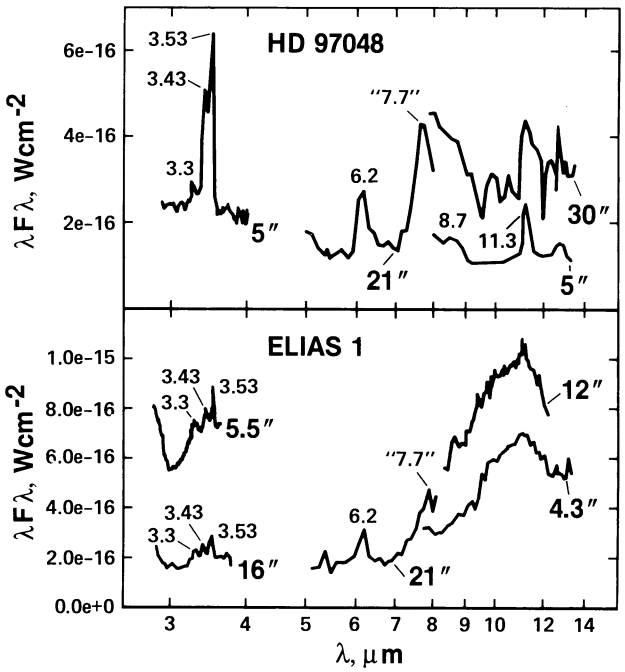

FIG. 3.—Summary of the spectral observations of HD 97048 and Elias 1 (21″, 12″, 16″, this paper; 5″.5, Whittet, McFadzean, and Geballe 1984; 4″.3, Whittet *et al.* 1988; 5″, Aitken and Roche 1981; 30″, *IRAS* LRS data base). The peaks are identified by wavelength, and the aperture size is indicated for each spectral data set.

data shown in Figure 3 were obtained allow us to determine the spatial distribution of the various emission features. Additional information on the spatial properties was obtained by speckle interferometry of the 3.53 μm feature of HD 97048, which showed that this feature originates from the inner $\sim$0.″05 around the stellar source (Roche, Allen, and Bailey 1986), corresponding to $\sim$10 AU (Thé *et al.* 1986). Since the 3.43 and the 3.53 μm features always appear together, we assume that they correlate spatially as well. This is supported by observations of HD 97048 which show no evidence of extension greater than 2″ for either feature (Baas *et al.* 1983). While the 3.43 and 3.53 μm features are spatially confined to a region of less than 0.″05 around HD 97048, inspection of Figure 3 shows that all the other emission features appear to be extended on at least a 20″ scale. For example, the fluxes in the "7.7"/8.7 and 11.3 μm features are more than two times larger in the spectrum from the *Infrared Astronomical Satellite* (*IRAS*) Low Resolution Spectra (LRS) data base (aperture $\approx$ 30″) than in the ground-based data (5″). Likewise, the KAO flux at 8 μm (21″) is about twice that observed from the ground (5″) and about 50% less than observed by *IRAS*. These differences are too large to be due calibration errors and are consistent with an extended origin of the family of well-known IR bands. Thus, although the 3.43 and 3.53 μm features are similar in shape to the normal IR emission bands and although they have never been observed without them, they seem to require very special conditions (i.e., the carrier must be close to the illuminating star) to be excited.

Figure 4 (*top*) shows a composite spectrum of HD 97048 using our observations and those of Aitken and Roche (1981). The KAO spectra, taken with a 21″ aperture, were scaled down to the 5″ aperture used by Aitken and Roche by multiplying the flux level by 0.55 to achieve an overlap at 8 μm. For comparison, a "typical" emission band spectrum is also shown in Figure 4 (i.e., Orion position 4; *bottom*). For Orion the 21″, 5–13 μm data were scaled to the 5″, 2.8–3.6 μm flux level by multiplying by 0.072 (Cohen *et al.* 1986). The anomalous nature of the 3.43 and 3.53 μm bands is readily apparent from Figure 4: they dwarf the other features.

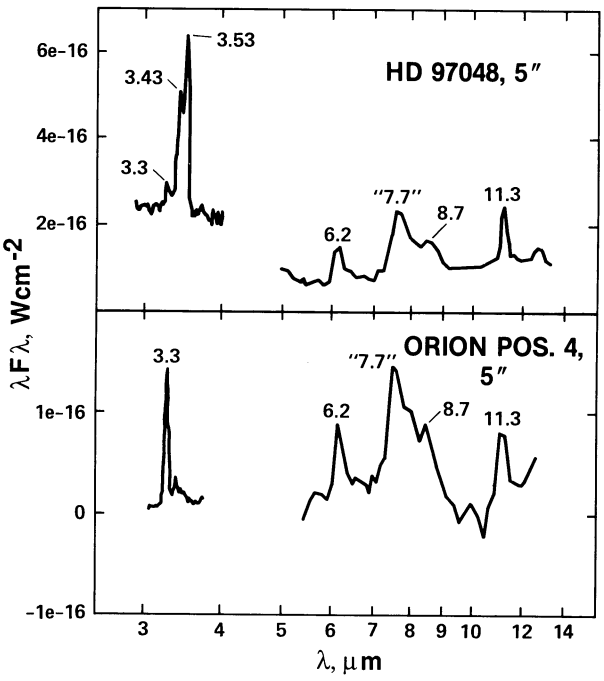

FIG. 4.—The 3–13 μm spectra of HD 97048 and Orion position 4, normalized to a 5″ aperture (see text; Orion: 3–4 μm, Geballe *et al.* 1989*b*; 5–14 μm, Bregman *et al.* 1989; HD 97048: 3–4 μm and 8–14 μm, Aitken and Roche 1981; 5–8 μm, this paper).

No attempt was made to produce a composite spectrum for Elias 1, since the emission by the "7.7" μm feature and the 10 μm silicate band, which both contribute to the flux in the overlap region, could have a very different spatial distribution and produce misleading results. Moreover, Elias 1 is variable (Elias 1978) and the IR spectrum suffers extinction by intervening ices. The most striking aspect of Figures 3 and 4 is the large intensity of the 3.43 and 3.53 μm features in comparison with the usual IR band family. Generally, the integrated intensity of all of the emission features in the 3 μm region of the spectrum (mainly the 3.3 μm feature) is only $\sim$10% of that at "7.7" μm (Cohen *et al.* 1986, 1989), whereas, in a 5″ aperture (see Fig. 4), the 3.43 and 3.53 μm features in HD 97048 emit together an amount of energy comparable to that in the "7.7" μm feature in a 21″ beam. Since the 3.43 and 3.53 μm bands actually originate within a 0.05″ aperture, the features should be even more dramatically enhanced with respect to the normal IR bands in such a small aperture.

The band positions, widths (FWHM), and integrated intensities (adjusted to 5″) of the emission features toward HD 97048 and Elias 1 are given in Table 1. The absolute intensities of the 3.43 and 3.53 μm bands towards HD 97048 were measured by Aitken and Roche (1981). However, the low resolution then available ($\sim$2%) was insufficient to separate the features and the relative intensities have been determined from the high-resolution data of Baas *et al.* (1983), who did not report absolute levels. A casual inspection of Table 1 and Figure 4 shows that the relative intensities of the normal IR bands at 3.3, 6.2, "7.7", 8.7, and 11.3 μm in HD 97048 and Elias 1 are very similar to those observed in other sources (Cohen *et al.* 1989). Thus, it seems that the IR emission spectra of HD 97048 and Elias 1 are produced by the carriers of the usual IR emission band family combined with an important additional component which contributes the 3.43 and 3.53 μm features.

b) Comparison to the 3 Micron Spectra of Other Astronomical Objects

The 3.43 and 3.53 μm emission bands of Elias 1 and HD 97048 are distinctly different from other interstellar emission and absorption features observed in this wavelength region. In Figure 5 the anomalous features of HD 97048 and HR 4049 (Baas *et al.* 1983; Geballe *et al.* 1989*a*) are compared to the 3.2–3.6 μm emission from Orion position 4 (Geballe *et al.* 1989*b*), the 3.4 μm absorption band observed toward the Galactic center (Butchart *et al.* 1986) and the 3.36 μm band emitted from the coma of comet Halley (Baas, Geballe, and Walther 1986). The differences in width and position between the 3.43 and 3.53 μm bands associated with HD 97048 and HR 4049 and these other interstellar emission and absorption features indicate that they originate from different classes of carriers. There is a suggestion of a peak match with weak bands in the Halley spectra. Likewise, there are very weak emission shoulders at about 3.43 and 3.53 μm in the spectra of the Orion bar.

The 3.2–3.6 μm region from objects that show the normal IR band family generally consists of a broad underlying plateau as

TABLE 1

CHARACTERISTICS OF THE EMISSION FEATURES TOWARD HD 97048 AND ELIAS 1

λ (μm)	ν (cm^{-1})	FWHM (μm)	FWHM (cm^{-1})	INTENSITY[a] (W cm^{-2})	RELATIVE INTENSITY[b]		REFERENCES
						generic[c]	
HD 97048							
3.3	3030	...	...	1.3 (−18)	0.11	0.08	1
3.434	2912	0.022	19	3.8 (−18)	0.32	...	1, 2
3.531	2832	0.023	18	8.3 (−18)	0.69	...	1, 2
6.2	1610	0.25	65	3.4 (−18)[d]	0.28	0.54	3
7.7	1300	0.6	100	1.2 (−17)[d]	1.00	1.00	1, 3
8.7	1150	0.7	90	5.6 (−18)	0.47	0.21	1
11.3	885	0.39	31	4.0 (−18)	0.33	0.29	1
Elias 1[e]							
3.29	3040	...	...	6.7 (−19)[f]	...	...	3
3.43	2915	0.04	34	6.9 (−19)[f]	...	...	3, 4
3.53	2833	0.03	24	1.3 (−18)[f]	...	...	3, 4
6.2	1610	0.25	65	5.3 (−18)[g]	...	...	3
7.9	1270	...	...	1.7 (−17)[g,h]	...	...	3

[a] Scaled to 5″ aperture.
[b] Normalized relative to the 7.7 μm feature.
[c] From Cohen *et al.* 1986 (for the 8.7 μm feature) and Cohen *et al.* 1989 (for the other features).
[d] Intensity at 21″ aperture was multiplied by 0.55 to scale to 5″ aperture (see text).
[e] No relative intensities are given for Elias 1, since scaling to a single aperture is impossible (see text).
[f] At 16″ aperture.
[g] At 21″ aperture.
[h] Flux shortward of 8 μm.
REFERENCES.—(1) Aitken and Roche 1981; (2) Baas *et al.* 1983; (3) this paper; (4) Whittet *et al.* 1984.

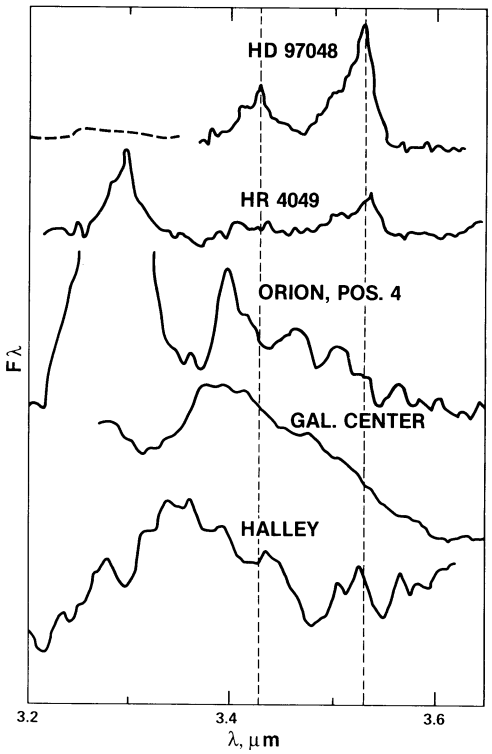

FIG. 5.—A comparison of the 3.43 and 3.53 μm emission features of HD 97048 and HR 4049 (Aitken and Roche 1981; Baas *et al.* 1983; Geballe *et al.* 1989*a*) to a number of other astronomical features; from top to bottom: the subfeatures in the 3.2–3.6 μm emission plateau toward Orion position 4 (Geballe *et al.* 1989*b*), the 3.4 μm absorption feature toward the Galactic Center source IRS 7 (Butchart *et al.* 1986), and the 3.36 μm emission band of the dust in the coma of comet Halley (Baas *et al.* 1986). The 3.3 μm spectrum of HD 97048 (*dashed line*) was taken from the low-resolution (2%) 2.8–4 μm data of Aitken and Roche (1981) and was scaled to the Baas *et al.* (1983) data by comparing the intensities of the 3.43 plus 3.53 μm features. The Galactic center absorption feature has, for convenience, been inverted.

well as a number of relatively weak emission features between 3.35 and 3.6 μm along with the 3.3 μm band (Geballe *et al.* 1985; de Muizon *et al.* 1986; Geballe *et al.* 1989*b*). The two most prominent subfeatures at 3.405 and 3.515 μm have been observed both toward planetary nebulae and H II regions. They are possibly due to overtones of the C-H stretching mode (Barker, Allamandola, and Tielens 1987, hereafter BAT; Geballe *et al.* 1989*b*). Although these peak at wavelengths different from the features of HD 97048 and Elias 1 (Fig. 5), they have weak shoulders at 3.425 ± 0.01 and 3.53 ± 0.01 μm, having intensities on the order of a few percent of the 3.3 μm feature. These bands seem to become relatively stronger in the intense UV field close to the H II region in the Orion nebula (Geballe *et al.* 1989*b*). The similarity in wavelength as well as in the apparent spatial distribution suggests perhaps that these very weak features might have an origin similar to the strong bands of HD 97048 and Elias 1. This notion is supported by the gradual transition apparent in Figure 5 from the case where the bands are very weak with respect to the 3.3 μm feature (Orion position 4), through the intermediate case (HR 4049) to the case where the bands dominate the 3.3 μm feature (HD 97048). It would be very interesting to observe these bands still closer to the Trapezium stars in Orion to test this suggestion and obtain a more solid basis for this comparison.

c) *Observational Constraints on the Carrier of the 3.43 and 3.53 Micron Emission Features*

Summarizing the above discussion, a number of properties of the carrier of the anomalous bands are apparent from the observations. The 3.43 and 3.53 μm features have been observed only under special conditions, i.e., close to a hot stellar source. Under less extreme conditions the 3.43 and 3.53 μm bands are, at best, only weak. In this respect it must be emphasized that, although the normal IR emission bands are generally attributed to UV-pumped IR fluorescence of molecules, this need not necessarily be true for the 3.43 and the

3.53 μm emissions. In view of the close proximity of the star, emission from hot dust grains in thermal equilibrium should also be considered. Moreover, due to the very intense UV field within the inner 10 AU around HD 97048 from which the anomalous features originate, it is likely that the carrier is highly excited. Under such conditions the peak of the emission will be shifted to shorter wavelengths. This is consistent with the relative weakness of the emission by the carrier at longer wavelengths (5–13 μm). Furthermore, the extreme conditions in this region will likely result in high destruction rates for a great number of species, constraining the number of candidates. Finally, the similar bandwidth, the fact that the three objects where they are observed also show the general IR emission bands, and the possible correspondence with some weak features in the generally observed 3.2–3.6 μm emission plateau suggest that the origin of the anomalous features may be related to the family of IR emission bands.

IV. POSSIBLE CARRIERS OF THE ANOMALOUS EMISSION BANDS

In the framework of the PAH hypothesis, two suggestions have been made to account for the spectroscopic structure in the 3.4–3.6 μm wavelength region: (1) vibrational modes of molecular sidegroups attached to the PAH skeleton (Duley and Williams 1981; de Muizon *et al.* 1986) and (2) higher order transitions (v = 2–1, 3–2, ...) of the C-H stretching mode or overtones and combination bands of C-C vibrations (BAT; Geballe *et al.* 1989*b*). In Figure 6 the anomalous features are compared to laboratory spectra of a number of these candidates. These assignments are discussed individually in detail below.

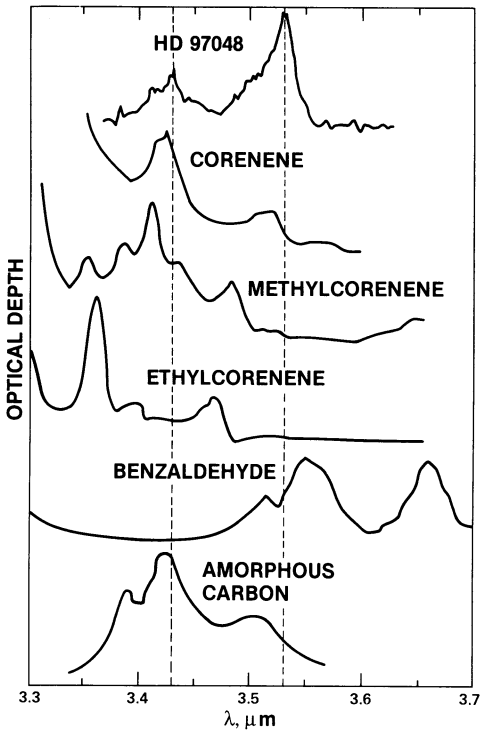

FIG. 6.—Comparison of the 3.43 and 3.53 μm features of HD 97048 (Baas *et al.* 1983) with a number of possible carriers. From top to bottom: the C-C overtone and combination bands of PAHs (in this case coronene; Cyvin and Klaeboe, reproduced in ATB87), the C-H stretching features of the sidegroups in methylcoronene [$C_{24}H_{11}(CH_3)$], d'Hendecourt and Léger 1987], ethylcoronene [$C_{24}H_{11}(CH_2CH_3)$], d'Hendecourt and Léger 1987], and benzaldehyde [$C_6H_5(CHO)$; Verlag Chemie GmbH Raman/IR Atlas] and the C-H symmetric and asymmetric stretching modes of $-CH_3$ and $-CH_2-$ molecular groups in amorphous carbon (Borghesi, Bussoletti, and Colangeli 1987).

a) Emission by Molecular (Side-)Groups

If the interstellar 3.43 and 3.53 μm bands are due to fluorescence from molecular sidegroups on PAHs or thermal emission of such groups in dust grains, their position is strongly suggestive of C-H stretching vibrations (Bellamy 1966). Because the frequency is diagnostic of the types of molecular sidegroups present, two possibilities can be distinguished, namely the C-H stretching mode of the aldehyde group ($-CHO$; van der Zwet *et al.* 1985) or of methyl ($-CH_3$) and methylene ($-CH_2-$) groups. Each possibility will be considered in turn.

Table 2 lists the positions and relative integrated cross sections of the main features of the $-CHO$, $-CH_3$, and $-CH_2-$ functional groups when attached to an aliphatic or aromatic carbon skeleton. For simplicity equal strengths for the methyl and methylene C-H vibrational stretching and deformation modes have been assumed. Table 3 lists absolute cross sections and positions for the general IR active modes of PAHs. Relative band strengths were compiled from spectra found in a number of sources. The absolute strengths listed in Table 3 were calibrated by adopting the integrated cross section of the 3.3 μm feature measured for PAH solids in KBr pellets (Léger, d'Hendecourt, and Défourneau 1989). For an extensive discussion of the IR modes of PAHs we refer to Allamandola, Tielens, and Barker (1989, hereafter ATB89).

i) *The Aldehydic C-H Stretch* ($-CHO$)

The aldehydic group produces two C-H stretching features with comparable intensities in the 3–4 μm region (Socrates 1980). Their positions and relative intensities, however, do not match the positions of the interstellar bands at 3.434 and 3.531 μm (Table 2; Fig. 6). It is perhaps possible, as was suggested by de Muizon *et al.* (1986) in a slightly different context, that aldehyde groups on ionized, partially dehydrogenated or electronically excited free molecular PAHs provide a better match.

Aldehydes all possess an intense, characteristic carbonyl (C-O) stretch in the 5.75–6.0 μm region (Table 2). The ratio of the integrated cross section of this band and that of the 3.67 μm C-H stretch is strongly phase-dependent; it is about 4 in the gas, 8 in the liquid, and 20 in the solid phase (in KBr; see Table 2). It does not seem to depend on whether the parent molecule is aliphatic or aromatic. Its absence in the observed 5–8 μm spectra (Fig. 1) argues against an aldehyde carrier.

To quantify this conclusion, we have calculated the relative intensities of the aldehydic C-H and C-O stretching features as a function of temperature, assuming thermal emission from large grains, and as a function of grain size and internal vibrational energy, assuming fluorescence from free PAHs (Fig. 7; BAT; ATB89; Schutte, Tielens, and Allamandola 1990). To be conservative, the lowest ratio of the integrated cross sections (i.e., gas phase) has been used in both cases. For comparison, the observational upper limits for HD 97048 and Elias 1 are also indicated (§ III).

Figure 7 shows that for HD 97048 even very hot grains or highly excited molecules give an expected C-O/C-H stretch intensity ratio that is considerably higher than the observed upper limit. If the internal vibrational energy of the PAH approaches infinity a Wien dependence of the emitted intensity is obtained (ATB89), giving the theoretical upper limit to this ratio of $\sim$0.6, still clearly above the observational upper limit.

TABLE 2

BAND POSITIONS, WIDTHS, AND RELATIVE CROSS SECTIONS INTEGRATED OVER WAVELENGTH FOR THE FUNDAMENTALS OF A NUMBER OF MOLECULAR SUBGROUPS[a]

VIBRATIONAL MODE	PHASE	PAH SIDEGROUPS			ALIPHATIC SUBGROUPS		
		Position (μm)	FWHM (μm)	Relative Integrated Cross Section (σ_{int}) (μm)	Position (μm)	FWHM (μm)	Relative Integrated Cross Section (σ_{int}) (μm)
				$-CH_3$[b,c]			
C-H asymmetrical stretch	Solid	3.407 ± 0.02	0.05 ± 0.02	1	3.383	0.02	1
C-H symmetrical stretch	Solid	3.490 ± 0.005	0.025 ± 0.01	0.4 ± 0.1	3.483	0.013	0.30 ± 0.08
C-H deformation	Solid	6.87 ± 0.02	0.10 ± 0.04	1.7 ± 0.4[d]	6.83	0.13	0.55 ± 0.14
		6.95 ± 0.03	0.11 ± 0.04	... ...	...	...	...
				$-CH_2-$[b,c]			
C-H asymmetrical stretch	Solid	3.369 ± 0.009	0.025 ± 0.009	1	3.422	0.03	1
C-H symmetrical stretch	Solid	3.48 ± 0.015	0.03 ± 0.01	0.4 ± 0.1	3.500	0.014	0.30 ± 0.08
C-H deformation	Solid	6.87 ± 0.02	0.1 ± 0.05	1.7 ± 0.4	6.83	0.13	0.55 ± 0.14
				−CHO			
C-H stretch	Solid	3.54 ± 0.02	0.07 ± 0.01	1.3 ± 0.7	...	...	...
	Liquid	3.54 ± 0.02	0.07 ± 0.01	1.1 ± 0.3	3.56 ± 0.01	0.07 ± 0.01	1.1 ± 0.3
	Gas	...	...	...	3.58 ± 0.01	0.07 ± 0.01	0.8 ± 0.2
C-H stretch	Solid	3.66 ± 0.02	0.04 ± 0.01	1	...	...	...
	Liquid	3.66 ± 0.02	0.04 ± 0.01	1	3.685 ± 0.01	0.07 ± 0.01	1
	Gas	...	...	...	3.685 ± 0.01	0.07 ± 0.01	1
C-O stretch	Solid	5.95 ± 0.04	0.07 ± 0.01	21 ± 6	...	...	...
	Liquid	5.89 ± 0.02	0.07 ± 0.01	7.5 ± 1	5.80 ± 0.05	0.12 ± 0.05	7.5 ± 1.0
	Gas	...	...	...	5.80 ± 0.05	0.12 ± 0.05	3.7 ± 0.6

[a] Spectra were obtained from the Sadtler Atlas, the Verlag Chemie GmbH Raman/IR Atlas, and from d'Hendecourt and Léger 1987, unless otherwise noted. Listed parameters for solids were measured in KBr and KI pellets, unless otherwise noted.

[b] Relative intensities of the C-H stretching and deformation modes of the $-CH_3$ group on one hand and the $-CH_2-$ group on the other hand were assumed equal.

[c] The aliphatic data were obtained for pure solids (d'Hendecourt and Allamandola 1986).

[d] Integrated cross sections of the two C-H deformation features were added.

TABLE 3

BAND POSITIONS, WIDTHS, AND INTEGRATED CROSS SECTIONS FOR PAH VIBRATIONS[a]

Mode	Condition	Position (μm)	FWHM (μm)	Integrated Cross Section (σ_{int}) (cm^2 μm)
C-H stretch	Solid	3.275 ± 0.01	0.03 ± 0.015	1.4 (−21)
	In neon	...	...	1.4 (−21)
C-C overtone comb. modes[b]	Solid	3.420 ± 0.006	0.031 ± 0.003	5.4 (−23)[c] 8.6 (−23)[d]
	Solid	3.514 ± 0.005	0.022 ± 0.003	1.7 (−23)[c] 2.0 (−22)[d]
C-C stretch	Solid	6.22 ± 0.05	0.05 ± 0.025	7.8 ± 2 (−22)
	In neon	...	...	7.6 (−22)
C-C stretch[b]	Solid	7.56 ± 0.25	0.065 ± 0.035	1.8 ± 0.4 (−21)
	In neon	...	...	2.0 (−21)
C-H bend (in plane)	Solid	8.45 ± 0.3	0.05 ± 0.02	1.4 ± 0.4 (−21)
	In neon	...	...	1.0 (−21)
C-H bend (out of plane)	Isolated C-H bond; solid	11.38 ± 0.1	0.1 ± 0.03	1.5 ± 0.9 (−19)
	Gas	...	...	4.0 (−20)
	Two adj. C-H bonds; solid	11.95 ± 0.1	0.16 ± 0.03	4.8 ± 2.5 (−20)
	In neon	...	...	1.9 (−20)
	Three adj. C-H bonds; solid	13.3 ± 0.5	0.18 ± 0.1	5.0 ± 2.5 (−20)

[a] Spectral data in the solid were measured in KBr and KI pellets and were obtained from the Sadtler Atlas; the Verlag Chemie GmbH Raman/IR Atlas; Cyvin and Klaeboe 1988; Cyvin *et al.* 1982; Donn 1988; Salisbury *et al.* 1988; and Léger, d'Hendecourt, and Défourneau 1989. Data in neon matrices were measured for coronene (Léger, d'Hendecourt and Défourneau 1989). The gas phase data were obtained for anthracene by H. Niki (1989, private communication). The relative band strengths measured from the spectra were converted to absolute strengths applying the integrated cross section of the 3.3 μm feature measured in KBr pellets (Léger, d'Hendecourt, and Défourneau 1989). Integrated cross sections are given per H atom for C-H vibrational modes and per C atom for C-C vibrational modes.

[b] Not found in the spectra of smaller PAHs ($\lesssim$24 C atoms).

[c] For coronene in KBr (Cyvin and Klaeboe 1988; Cyvin *et al.* 1982).

[d] Minimum strength required for producing the anomalous 3.43 and 3.53 emission features toward HD 97048 (see text).

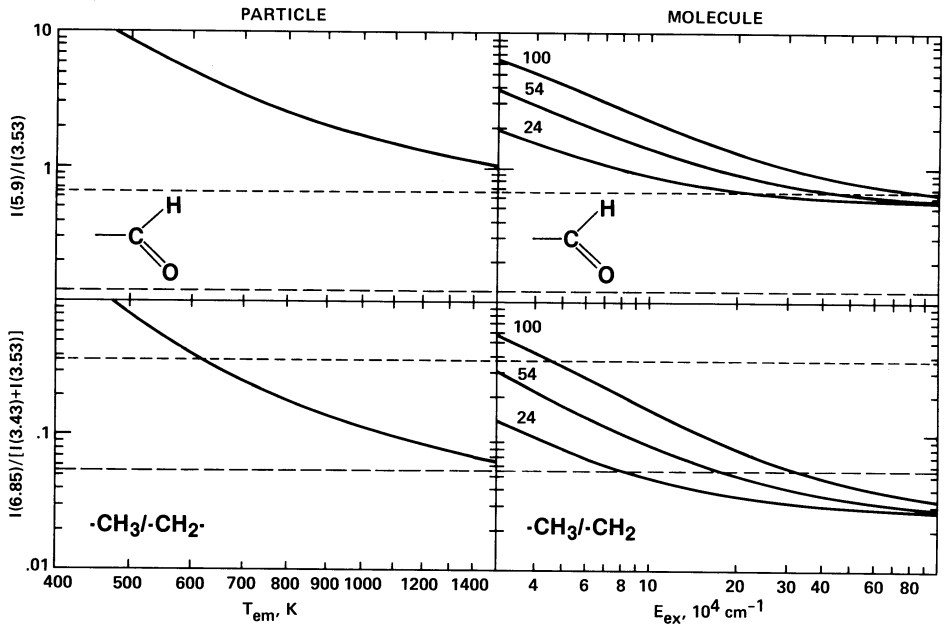

FIG. 7.—The calculated emission intensity ratio of the C-O stretching band near 5.9 μm to the longest wavelength C-H stretching band for the aldehydic —CHO group, and of the emission intensity ratio of the C-H deformation mode near 6.85 μm to the stretching mode (symmetric + asymmetric) for the methyl (—CH_3) and methylene (—CH_2—) groups. Results are shown for two cases: that of thermal emission by particles and that of fluorescence from sidegroups on isolated PAH molecules. For the particle case, results are plotted as a function of temperature, while for the molecule case, the results are plotted against internal vibrational energy. The fluorescence was calculated for PAH molecules with aromatic skeletons having 24, 54 and 100 carbon atoms. Observational upper limits of the ratios for HD 97048 (*wide dashed line*) and Elias 1 (*narrow dashed line*) were obtained from the data displayed in Fig. 1, assuming that the 3.43 and 3.53 μm features can be assigned to the C-H stretching modes of —CHO or —CH_3/—CH_2—. For details see text.

For Elias 1 there is a possibility that highly excited PAHs with aldehyde sidegroups could produce the 3.53 μm emission feature without producing a detectable C-O stretching feature at 5.75–6.0 μm (Fig. 7). However, the similarity in position and profile of the emission features from Elias 1 to the features from HD 97048 (Whittet, McFadzean, and Geballe 1984) argues against a different origin in this source.

In conclusion, assigning the 3.43 and 3.53 μm emission features to the —CHO group, either as a sidegroup on PAHs or as a part of grains, is very unlikely due to the absence of a clear carbonyl band between 5.75–6.0 μm and the mismatch of the aldehyde features with the interstellar bands.

ii) *The Aliphatic* C-H *Stretch* (—CH_3, —CH_2—)

Methyl (—CH_3) and methylene (—CH_2—) groups produce an asymmetric and a symmetric C-H stretching feature in the 3–4 μm region. The positions of the bands are considerably different if the groups are part of an aliphatic group or if they are sidegroups on an aromatic moiety (see Table 2). Figure 6 compares laboratory spectra of the symmetric and asymmetric C-H stretching region of —CH_3 and —CH_2— with the 3.3–3.6 μm spectrum of HD 97048. These spectra include samples with sidegroups on PAHs as well as an amorphous carbon material, a solid mixture of aromatic and aliphatic structures (Borghesi, Bussoletti, and Colangeli 1987). The features of the amorphous carbon are due to —CH_3 and —CH_2— groups in aliphatic chains as well as on PAHs, where the former seem to dominate given the measured peak positions and relative strengths (see Fig. 6 and Table 2). Although —CH_3 and —CH_2— sidegroups on PAHs give a somewhat better match than the C-H stretching mode in aldehyde groups (Fig. 6), there remains a significant discrepancy in position and relative band strength. As for the aldehydic sidegroups, the discrepancy could possibly be due to ionization or excitation of the PAHs. On the other hand, the band peak positions are reasonably well matched by the IR bands of the amorphous carbon. However, the shorter wavelength asymmetric stretching feature is considerably stronger than the longer wavelength symmetric stretching band in this material, contrary to what is observed. Furthermore, the asymmetric C-H stretching band of the amorphous carbon is split into two bands, i.e., the 3.43 μm —CH_2— and the 3.39 μm —CH_3 feature. The —CH_3 feature seems to be absent in the observed 3.43 μm emission feature of HD 97048. Thus, if one ascribes the anomalous bands of HD 97048 to amorphous carbon, it must have little —CH_3 groups relative to —CH_2— groups, indicating the dominance of long linear chain molecules. Note that, in contrast, the best data currently available on the 3.4 μm absorption feature of interstellar carbon grains, i.e., toward the Galactic center source IRS 7, display a clear —CH_3 as well as —CH_2— asymmetric stretching feature, apparently indicating comparable abundances of —CH_3 and —CH_2— groups (see Fig. 5; Butchart *et al.* 1986).

Besides the IR active C-H symmetric and asymmetric stretching modes at 3.4–3.5 μm, methyl and methylene groups have strong IR active deformation modes near 6.8 μm. For —CH_3 sidegroups on PAHs, the 6.8 μm band splits into two features separated by about 0.08 μm. The strength of the deformation relative to the stretching mode seems to be strongly influenced by the nature of the carbon skeleton. It is about 3 times stronger in aromatic than in aliphatic compounds. A similar effect has been found for —CH_2— and —CH_3 groups adjacent to C—C bonds (Wexler 1967). No apparent dependence of the relative band strengths on phase has been reported (Wexler 1967).

The apparent absence of the C-H bending mode at 6.8–6.9 μm in the astronomical spectra (Fig. 1) provides a further constraint on the —CH_3/—CH_2— assignment. In Fig. 7 the ratio of the intensity of the C-H bending mode to the intensity of the

combined symmetric and asymmetric C-H stretching modes is plotted as a function of emission temperature, or vibrational energy, for thermal emission by grains and for fluorescence from sidegroups on free molecular PAHs, respectively. To be conservative, the ratio of the integrated cross sections of the bending to the stretching mode was taken equal to the aliphatic value of 0.4 (Table 2). Again, observational upper limits for HD 97048 and Elias 1 are also plotted (§ III). Considering Figure 7, it seems that the nondetection of a distinct feature in the 6.8 μm region cannot rule out a $-CH_3/-CH_2-$ assignment, if the emitting material is either highly excited (molecule: $E \gtrsim 2 \times 10^5$ cm^{-1}) or has a high emission temperature (particle: $\gtrsim$1500 K). For example, at a distance of 8 AU from the stellar source, the PAH molecule $C_{54}H_{17}(CH_3)$ will have a mean vibrational energy content of about 2.5×10^5 cm^{-1} (Schutte, Tielens, and Allamandola 1990), and an emission spectrum consistent with the observational upper limit of the C-H deformation to C-H stretch intensity ratio. Likewise, the implied high temperature of thermally emitting dust grains ($\gtrsim$1500 K) is not impossible given the observed high continuum dust temperature inferred for this source (Thé *et al.* 1986). It must be kept in mind, however, that if a ratio of the intensity of the combined stretching bands to the intensity of the deformation band of about unity had been taken, as appropriate for aromatic substances (see Table 2), the 6.8 μm band upper limit would rule out $-CH_3$ and $-CH_2-$ sidegroups on PAHs. Both the fluorescence and thermal emission model predict C-H bending mode intensities not too far below the detection limit. Therefore, future higher signal-to-noise ratio 5–8 μm observations may be able to put stronger observational constraints on the $-CH_3/-CH_2-$ assignment.

An important additional constraint on the assignment of the anomalous 3.43 and 3.53 μm features to thermal emission by $-CH_3/-CH_2-$ groups in dust particles is the stability of such material at high temperatures. In order to emit efficiently at 3.43 μm, the particles should have a temperature of at least $\sim$800 K ($T \approx 0.3/\lambda$). As deduced above, the emission temperature of the dust required to match the observed upper limit of the 6.8 μm C-H deformation to 3.43 and 3.53 μm intensity ratio is even higher, i.e., more than 1500 K. However, aliphatic molecules are not stable at these temperatures. Aliphatic hydrogen atoms are driven off and the carbon atoms rearrange into aromatic domains when amorphous carbon is heated to temperatures in excess of about 700 K for periods longer than 1 hr (Mortera and Low 1983; Borghesi, Bussoletti, and Colangeli 1987). The 3.43 and 3.52 C-H stretching features completely disappear in this process, arguing strongly against thermal emission by aliphatic groups in hydrogenated amorphous carbon grains as the explanation of the anomalous features. This stability argument does not necessarily hold for a model based upon sidegroups on free molecular PAHs since, in that case, the emission may be "nonthermal" in nature and temperature is ill defined. The loss of sidegroups then has to be calculated using a microcanonical description (i.e., RRKM theory; Tielens *et al.* 1987, hereafter TABC; ATB89).

Summarizing, although thermal emission by $-CH_3/-CH_2-$ groups in amorphous carbon grains can produce a reasonably good fit to the peak positions of the interstellar 3.43 and 3.53 μm band, the relative strengths of the bands are difficult to rationalize. More importantly, such an assignment seems unlikely since laboratory studies show that amorphous carbon will lose its aliphatic hydrogen rapidly at the required high emission temperatures. Although a nonthermal model based on fluorescence of aliphatic groups connected to the PAHs might circumvent this problem, the 3 μm spectra of PAHs with sidegroups do not fit the observed spectra.

b) PAH Hot Bands, Overtone, and Combination Bands

In this section the possibility that the 3.43 and 3.53 μm features are due to highly excited PAHs (without sidegroups) is investigated. In this case, the strong 3.43 and 3.53 μm bands may originate from hot band transitions of the C-H stretching mode in very highly excited molecules or from overtones and combination bands of the C-C stretching modes (BAT). We will discuss each of these possibilities in turn.

i) *Hot Band Transitions of the* C-H *Stretching Mode*

Emission in the 3 μm region from interstellar PAHs is generally characterized by a broad plateau with a number of superposed subfeatures along with the dominant 3.3 μm emission band (de Muizon *et al.* 1986; Geballe *et al.* 1989*b*; see Fig. 5). The two most prominent subfeatures fall at 3.405 and 3.515 μm and have been assigned to "hot bands" of the 3.3 μm C-H stretching mode ($v = 2$–1, $v = 3$–2; BAT; Geballe *et al.* 1989*b*). Although these bands fall at somewhat different wavelengths than the anomalous 3.43 and 3.53 μm bands, the discrepancy could be due to another class of PAHs being excited under the extreme conditions in the emission region close to the stellar object. However, there are a number of arguments against this assignment of the anomalous emission features. First, there is no sign of the $v = 4$–3 transition expected near 3.6 μm which should be very intense in view of the strength of the 3.53 μm band. Additionally, the intensity of the 3.43 and 3.53 μm features relative to the fundamental at 3.3 μm is, in this model, limited to the ratio of the Einstein A-values (about 2 and 3 respectively; BAT; ATB89). Yet, the 3.53 μm feature is observed to be about 6 times as intense as the 3.3 μm feature in HD 97048 (Table 1; see also Fig. 4) and in view of the spatial data, the actual 3.53/3.3 μm ratio within 0.″05—the site of the 3.53 μm feature emission zone—is probably even larger (see § III*a*). We conclude that the anomalous bands cannot be assigned to hot bands of the aromatic C-H stretching mode.

ii) *Overtones and Combination Bands of* C-C *Modes*

Laboratory spectra of pure PAHs show two weak absorption features near the positions of the anomalous interstellar features (Cyvin and Klaeboe, reproduced in Allamandola, Tielens and Barker 1987, hereafter ATB87; and in ATB89). These bands have been ascribed to C-C overtone and combination bands. The position and shape of the features seem to be quite stable in the laboratory. For coronene ($C_{24}H_{12}$), benzopentaphene ($C_{24}H_{14}$), circodiphenyl ($C_{38}H_{16}$), and hexabenzocoronene ($C_{42}H_{18}$) in KBr, the bands lie between 3.41–3.43 and 3.51–3.52 μm (Donn 1988; Salisbury *et al.* 1988). Weak shoulders on the 3.41 and 3.51 μm CH "hot" bands have indeed been observed in several interstellar objects near these wavelengths and were ascribed to overtones and combination bands of C-C modes (BAT; Geballe *et al.* 1989*b*). In Figure 6 the bands of coronene suspended in KBr are compared to the anomalous features of HD 97048. The PAH bands fit the anomalous features reasonably well in both position and width. In spite of the slight discrepancy in wavelength, we will, for convenience, also refer to these weak laboratory bands as the "3.43" and "3.53" μm features, after the anomalous interstellar features. In the laboratory, the longer wavelength feature is weaker than the shorter wavelength band, contrary

to what is observed. In the laboratory spectra the strength of the 3.43 μm band is quite likely amplified with respect to the 3.53 μm band by Fermi resonance of this feature with the strong 3.3 μm C-H stretching mode (Herzberg 1945). Since the emitting interstellar PAHs are expected to have a very low hydrogen-to-carbon ratio (see below), this objection may therefore not be too worrisome. We conclude therefore that the best explanation (rationalization?) of the anomalous features is in terms of overtones and combination bands of C-C stretching vibrations in the larger PAHs which survive in the emission zone.

iii) *The Model*

Within the framework of the proposed assignment to C-C bands, the anomalous intensities of the interstellar 3.43 and 3.53 μm features relative to the 3.3 μm band implies that these features must be emitted by PAHs with extremely low H-to-C ratios. Naively extrapolating from the coronene 3.53/3.3 μm ratio listed in Table 3 (these bands are used to minimize any Fermi resonance interference) to the observed ratio we estimate that the H/C ratio of the carrier is at most of the order 3×10^{-3}. One possibility is that the bands are emitted by very large PAHs, since the C-to-H ratio of compact PAHs is roughly proportional to $N_C^{1/2}$, the square root of the number of carbon atoms in the PAH. Alternatively, or possibly additionally, the bands may be emitted by completely dehydrogenated PAHs. Since the relative strength of the 3.43 to the 3.53 μm feature in the laboratory spectra may have been influenced by a Fermi resonance of the former with the 3.3 μm C-H stretch, dehydrogenated or large PAHs may also provide a better fit to the observed 3.43/3.53 μm ratio. Furthermore, the high intensity of the 3.43 and the 3.53 μm band relative to the 6.2 and 7.7 μm features which are due to the C-C fundamentals toward HD 97048 compared to that generally observed (e.g., Orion position 4; see Fig. 4) suggests that the PAH emitters of these features must be considerably more vibrationally excited than under "normal" conditions (§ III*c*). All of these constraints seem consistent with the high energy densities expected in the emission region close to the star. PAHs will be highly vibrationally excited here, and the smaller PAHs may be dehydrogenated or even destroyed by the intense UV field (TABC).

Close to the star, multiphoton processes (i.e., absorption of one or more UV photons before the energy of a previously absorbed photon has been radiated away) play an important role in the excitation, dehydrogenation, and destruction processes of the PAH molecules. For example, within a typical radiative cooling time scale of $\sim$2 s (ATB89), a 20 C atom PAH will absorb about 3 UV photons (corresponding to a total energy of about 25 eV) at a distance of 20 AU, the border of the observed emission zone of the 3.53 μm feature. Unimolecular dissociation of a highly vibrationally excited PAH, leading to H loss or rupture of the C skeleton, will occur when sufficient energy is located within a particular bond (i.e., a C-H or a C-C bond, respectively). The internal vibrational energy required for bond dissociation increases considerably with the size of the PAH, since larger PAHs have more vibrational modes over which they can distribute the energy. For carbon atom ejection, at least two adjacent bonds need to be broken simultaneously, so that a considerably larger internal energy is required to induce C loss than to induce H loss. For PAHs larger than $\sim$30 C atoms, the threshold for H loss is more than 13.6 eV, the Lyman limit, and multiphoton processes are then required if even H is to be eliminated. For all relevant PAH sizes, rupture of the C skeleton requires multiphoton processes (TABC; ATB89).

From this a picture emerges of the distribution of PAH chemical states at various distances from the star. Figure 8 gives a schematic representation of the different zones into which the circumstellar environment can be divided corresponding to the chemical state of the PAH molecules. The outer zone (zone I) contains "normal", ionized, hydrogenated PAHs, which emit the absorbed UV energy in the 3.3, 6.2, "7.7," 8.7, and 11.3 μm features. Large, highly excited PAHs will also contribute to the 3.43 and 3.53 μm features. In this zone the rate of hydrogenation of PAHs by the ambient atomic hydrogen flux is larger than the dehydrogenation rate by the UV photon field. For PAHs containing more than $\sim$30 C atoms, hydrogen loss requires multiphoton absorption processes. The probability of multiphoton events increases rapidly at closer distance to the exciting star. Thus, below a specific stellar distance, the PAHs will start to become dehydrogenated (zone II), until, finally, only PACs (polycyclic aromatic carbons, i.e., dehydrogenated PAHs) remain (zone III). The PACs will emit their absorbed energy exclusively in the 3.43, 3.53, 6.2 and "7.7" μm features. Finally, even closer to the star, the PAH skeletons will be destroyed when they get sufficiently excited by the extremely high rate of UV photon absorptions. Note that the dehydrogenation and destruction distances are smaller when the PAHs are larger, as they must absorb a larger number of photons before hydrogen loss or ring break-up and carbon loss can occur (TABC). Modeling of this process indicates that PAHs or PAH clusters containing more than 500–1000 C atoms will survive within the inner $\sim$10 AU emission zone (Schutte, Tielens, and Allamandola 1990). Thus, the emission from close by the exciting star will be dominated by highly excited, (de)hydrogenated, large PAHs or PAH clusters.

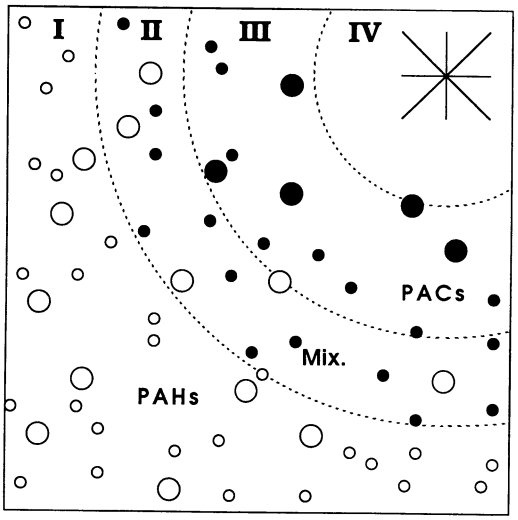

FIG. 8.—Schematic of the condition of the PAH type distribution in the region around HD 97048. In zone I the PAHs have peripheral H atoms (*empty circles*). Closer to the exciting stellar object, the PAHs become dehydrogenated by multiphoton processes (zone II), i.e., become PACs (*filled circles;* PAH + $n*h\nu \rightarrow$ PAC + $m*$H), until finally all PAHs are dehydrogenated (zone III). The PAHs emit the 3.3, 6.2, "7.7," 8.7, 11.3 μm features as well as some of the observed 3.43 and 3.53 μm bands while the PAC emission produces only features at 3.43, 3.53, 6.2, and "7.7" μm. Finally, still closer to the central star, the high energy density of the radiation field will destroy the carbon skeletons (zone IV). Note that the dehydrogenation and destruction take place closer to the star for larger PAHs. For details, see text.

The required intrinsic strengths of the 3.43 and 3.53 μm large PAH (or PAC) bands can be constrained by their intensities relative to the 6.2 and "7.7" μm features. For the highly excited PAHs within the 0".05 ($\sim$10 AU) emission zone around HD 97048, a Rayleigh dependence of the emission is expected (Schutte, Tielens, and Allamandola 1990), and the observed intensities of the 3.43 and 3.53 μm features relative to the 6.2 μm emission feature (see Table 1) indicate intrinsic band strengths of, respectively, 0.11 and 0.26 relative to the 6.2 μm feature. When adopting the 6.2 μm strength of 7.8×10^{-22} cm^2 μm (Table 3), this yields integrated strengths of 8.2×10^{-23} cm^2 μm and 2.0×10^{-22} cm^2 μm for the 3.43 and 3.53 μm features, respectively. Since a large fraction of the 6.2 μm feature observed within a 5" aperture is likely emitted outside of the 0".05 emission zone of the anomalous bands, these strengths should be regarded as lower limits. For coronene, the strength ratio of the 3.43 and 3.53 μm features relative to the 6.2 μm feature was measured in KBr, giving 0.07 and 0.02, respectively (see Table 3). Evidently, the PAHs near HD 97048 need to have a more than 10 times stronger 3.53 μm C-C feature than coronene. The 3.43 μm feature, which, for coronene, is likely strengthened by Fermi resonance, needs an enhancement of about a factor of 2. Possibly, the enhancement of the 3.43 and 3.53 μm features could be due to the much larger size of the PAHs emitting from the circumstellar zone (i.e., $>$500–1000 C atoms). This is reasonable from a spectroscopic point of view. As the large molecules become more and more complex and less symmetric, the symmetry selection rules, which determine the different intrinsic band strengths of fundamentals and overtone and combination bands, break down and weak transitions can become stronger with respect to the (already strong) fundamentals. This symmetry break down also occurs as molecules become more excited. For example, symmetry selection rules applied to benzene predict that all even numbered overtones of the C-H skeleton ($2 \rightarrow 0$, $4 \rightarrow 0$, ...) should not be infrared active (Wilson, Decius, and Cross 1955). However, these transitions are observed to be quite strong in highly excited benzene (Reddy, Heller, and Berny 1982). Thus, both conditions which are required to enhance the strength of the overtone and combination bands with respect to the fundamentals are met in the emission zone around HD 97048.

Calculating the column density of the carbon in the PAHs toward HD 97048 from the observed flux in *all* IR emission bands and using $A_V = 0.34$ mag to calculate the column density of carbon in the circumstellar shell (Thé *et al.* 1986), it follows that the PAHs near HD 97048 contain on the order of 3% of the available carbon. This is comparable to the abundances found in other sources (Léger and d'Hendecourt 1987; Chlewicki and Laureijs 1988; Bregman *et al.* 1989; ATB89).

Summing up this section, we conclude that the intensities of the 3.43 and 3.53 μm features observed toward HD 97048 can be reproduced if the C-C overtone and combination bands in large PAHs have strengths of at least 0.11 and 0.26, respectively, times that of the 6.2 μm C-C mode.

iv) *Comparison with Other PAH Sources*

In most objects which emit the common IR band spectrum PAHs in the 20–30 C atom size range with 10–15 H atoms are thought to be responsible for the 3.3 μm feature (ATB87; BAT). For such PAHs the strengths of the 3.43 and 3.53 μm modes should be much smaller than those of the large, highly excited PAHs toward HD 97048. For example, towards Orion position 4 the intensities of the very weak shoulders are about 3% and 2%, respectively, of the 3.3 μm feature (Geballe *et al.* 1989*b*). Since the 3.3, 3.43, and 3.53 μm features should be almost equally excited due to their proximity in excitation energy, this indicates strengths of the 3.43 and 3.53 μm features which are comparable to those measured for coronene in KBr (8% and 2%, respectively, of that of the 3.3 μm feature; see Table 3). Thus, per C atom, the intrinsic strengths of the 3.43 and 3.53 μm features of the PAHs at Orion position 4 are, respectively, 4 and 10 times less than the minimum required strengths for the PAHs towards HD 97048.

Within this framework, strong emission in the anomalous 3.43 and 3.53 μm C-C bands requires large PAHs, as the strength of these features compared to the other bands are too weak in the smaller PAHs thought to be the usual emitters of the IR bands in the 3 μm region. Excitation of such large PAHs requires multiphoton processes. This is only expected to occur in the vicinity of a hot star. For example, as noted above, a PAC or PAC cluster of 500 C atoms within 10 AU from HD 97048 will have a Rayleigh dependence for the IR band emission, and intrinsic band strengths of 0.11 and 0.26 are then required for the 3.43 and 3.53 μm features relative to the 6.2 μm band to obtain the observed relative intensities, i.e., the emitted intensity in the 3.43 plus the 3.53 μm feature is 3 times larger than in the 6.2 μm band. At 30 AU, with these intrinsic strengths, such a PAC would emit 1.2 times more flux in the 3.43 plus the 3.53 μm band than in the 6.2 μm feature. At 100 AU this intensity ratio has dropped to 0.15. If the PAC becomes hydrogenated, the intensity emitted in the anomalous bands will be even lower, since the hydrogenated PAH has more vibrational modes over which to distribute the energy, and it can emit at more frequencies. It can thus be concluded that, within our model, large PAHs or PACs must be abundant within 10–100 AU from a hot stellar source (depending on the stellar luminosity) in order to give rise to anomalously intense 3.43 and 3.53 μm emission features. This requirement is met only when the illuminating stellar object is surrounded by a circumstellar shell or an accretion disk.

A search for 3 μm features toward Herbig Ae/Be stars was made by Allen *et al.* (1982) and Whittet *et al.* (1983). A survey of 39 such objects did not turn up any other anomalous 3.43 and 3.53 μm bands, while only two other objects showed the 3.3 μm feature. No correlation between the presence of emission features and spectral type was found. Thus it seems that only a small fraction of Herbig Ae/Be stars shows anomalous IR band emission. This implies that either the majority of these stars do not have circumstellar material sufficiently close to the star to excite the anomalous 3.43 and 3.53 μm features or that their circumstellar material is poor in large PAH molecules. The absence of considerable amounts of any circumstellar PAHs seems necessary to account for the nondetection of any 3 μm emission feature in the spectra of most of the Herbig Ae/Be stars.

In addition to young stellar objects, the requirement of large PAHs close to an exciting star might be met by mass losing carbon stars. Normal C-rich giants are thought to form copious amounts of carbon dust and presumably PAHs (ATB89; Frenklach and Feigelson 1989). However, the UV flux of these cool stars ($\sim$2500 K) is much too low to ionize and excite the PAHs. However, objects in the transition phase from mass-losing carbon star to planetary nebula may both be sufficiently hot to emit large amounts of UV flux as well as have carbon-rich material sufficiently close to the star to show emis-

sion in the 3.43 and 3.53 μm features. Indeed, HR 4049, which is believed to be a carbon-rich, low-mass star, with a high mass-loss rate that is evolving into a planetary nebula, shows a distinctive 3.53 μm feature and probably also a 3.43 μm band (Geballe *et al.* 1989*b*; see Fig. 5). An interesting difference between this object and HD 97048 is that the ratio of the intensity of the anomalous bands to the 3.3 μm feature is about one-tenth of that of HD 97048. In our model, this indicates that the PAHs are farther out relative to the exciting star in HR 4049. Perhaps, this difference is related to the different phases of stellar evolution that HD 97048 and HR 4049 are thought to represent. It would be very interesting to investigate further the spatial distribution of the anomalous features as well as of the general family of IR emission features towards these sources.

Another well-known example of a hot star ($\sim$10,000 K) associated with carbon-rich outflow is HD 44179, the Red Rectangle. However, although this object emits the well-known IR emission bands within a 2".7 aperture, there is absolutely no sign of the aromatic 3.43 and 3.53 μm emission bands at a level higher than a few percent of the intensity of the 3.3 μm feature (Tokunaga *et al.* 1988). The evolutionary status of this object is not well known, but it probably is also a protoplanetary nebula. Since the outflow originates on or near the stellar surface, the absence of the 3.43 and 3.53 μm features is puzzling. Possibly, the hot star HD 44179 is illuminating the mass losing envelope of a (red giant) companion as suggested by recent near-infrared speckle studies (Leinert and Haas 1989). The projected distance (0".15) corresponds to 50 AU at the distance of this object (330 pc; Cohen *et al.* 1975), and it is possible that the emitting species are located much farther from the hot star than in the case of HD 97048.

v) *Summary*

If due to PAHs, the anomalous 3.43 and 3.53 μm features seem most likely due to overtones and combination bands of C-C stretching modes. Such an assignment is supported by the observation of weak shoulders near the anomalous band positions in some objects which show the general IR band spectrum as well as by weak bands corresponding to these modes near the correct positions in the laboratory spectra of PAHs. In this model, the anomalously high intensity of the 3.53 and 3.43 μm features relative to the normal features of the IR band family toward HD 97048 indicates that the emitting PAH species must be very highly excited and have an extremely large C/H ratio. These requirements are consistent with the conditions in the 3.53 μm band emission zone of $\sim$10 AU around the exciting star, where only large, possibly dehydrogenated, PAHs will be able to survive the high excitation induced by multiphoton absorptions. Comparison of the intensities of the anomalous 3.43 and 3.53 μm bands with the usual family of IR emission features for HD 97048 and for objects showing no anomalous emission, such as Orion position 4, indicates that the intrinsic strength of the anomalous features should be at least an order of magnitude stronger in the PAHs emitting around HD 97048. If this explanation is correct, this behavior may be due to the very large size of the PAHs supposed to be emitting the anomalous features, i.e., at least 500–1000 C atoms compared to 20–30 C atoms for the PAHs that usually emit in the 3 μm region. Thus the anomalous 3.43 and 3.53 μm emission can occur only if very large PAHs are highly excited, i.e., in the vicinity of a hot star.

V. CONCLUSIONS

Using new airborne observations in the 5–8 μm region, we have investigated the origin of the anomalous 3.43 and 3.53 emission features that are observed toward the objects HD 97048, Elias 1, and quite recently, HR 4049. Two possible assignments were considered, i.e., emission from molecular subgroups; either in dust particles or as sidegroups of PAH molecules, and emission by the C skeleton of PAH molecules. If due to vibrational modes of molecular (side-)groups, the position of the anomalous features point to C-H stretching modes. An assignment of the features to the C-H stretching modes of the —CHO group is ruled out by the absence of a carbonyl C-O emission feature between 5.75 and 6 μm and the poor peak position match. Similarly, the peak positions do not match the $-CH_2-$ and $-CH_3$ frequencies expected from sidegroups on PAHs. $-CH_2-$ and $-CH_3$ groups in amorphous carbon particles on the other hand give a reasonably good match to the positions of the anomalous features. However, the required high emission temperature ($\gtrsim$1500 K) rules against emission from amorphous carbon particles because such materials lose aliphatic groups and become graphitized on a time scale of hours at temperatures in excess of 700 K.

The physical conditions of high excitation in the emission zone (which is within about 10 AU from the exciting star, HD 97048), the fact that the anomalous features are always observed together with the general family of IR emission features, and the presence of similar but much weaker features that seem to be associated with the family of IR emissions suggest an assignment to PAH related material. An assignment to C-C overtone and combination bands in large ($\geq$500–1000 C atoms), possibly dehydrogenated, PAHs or PAH clusters is most likely. In the emission zone only PAHs containing more than 500–1000 carbon atoms can survive the high excitation caused by multiphoton absorptions from the intense stellar UV field. In this model, the cross sections for the overtone/combination bands of large species are required to be enhanced relative to their fundamentals. These large PAHs have high C-to-H ratios and may also be dehydrogenated, so that they will emit little in the 3.3 μm C-H stretch band with respect to the C-C modes. Farther out from the star, smaller, less excited PAHs can survive and produce the more general family of PAH IR emission bands.

In this model anomalously strong 3.43 and 3.53 μm bands are only expected in the presence of PAHs extremely close to a strong UV source, i.e., a hot stellar object. This can be either a protostellar object surrounded by a circumstellar accretion disk or shell or a mass-losing C-rich giant which is evolving into a planetary nebula. The short duration of the transition phase from mass-losing giant to planetary nebula may account for the uniqueness of HR 4049 among mass-losing objects in showing the anomalous features. The absence of anomalous emission features in the spectra of most hot protostellar objects could be due either to the absence of large PAHs in the circumstellar disk or shell or to the absence of circumstellar material sufficiently close to the star to excite the anomalous 3.43 and 3.53 μm features. The presence of these features may represent a relatively short-lived phase in the chemical or spatial evolution of the circumstellar accretion disk. An interesting test of the C-C overtone and combination band model of the anomalous emission features would be to study the spatial distribu-

tion of the 3.43 and 3.53 μm and the general family of IR emission features in the circumstellar material. This model predicts that the bulk of the emission from the 3.3 μm feature should originate outside the emission zone of the anomalous features, while part of the overall intensity of the 6.2 and "7.7" μm features must come from within this zone (see Fig. 8).

Finally, it should be stressed once again that more laboratory data on PAHs obtained under astrophysically relevant conditions are necessary to further investigate the connection between PAHs and the anomalous (as well as the general) IR emission features.

We thank the staff of the KAO for their indispensable assistance with our airborne observations. We gratefully acknowledge many valuable discussions with John Barker on modeling the PAH IR emission. We thank Alan Tokunaga for making his 3 μm spectral data toward Elias 1 available to us prior to publication and Amara Graps for her assistance in reducing the Mount Lemmon data. This research was supported by NASA grant 188-41-57 from the Infrared/Radio Astrophysics Branch.

REFERENCES

Aitken, D. K., and Roche, P. F. 1981, *M.N.R.A.S.*, **196**, 39P.
Allamandola, L. J., Bregman, J. D., Sandford, S. A., Tielens, A. G. G. M., Witteborn, F. C., and Wooden, D. H. 1989, *Ap. J. (Letters)*, **345**, L59.
Allamandola, L. J., Tielens, A. G. G. M., and Barker, J. R. 1985, *Ap. J. (Letters)*, **290**, L25.
———. 1987, in *Physical Processes in Interstellar Clouds*, ed. G. E. Morfill and M. Scholer (Dordrecht: Reidel), p. 305 (ATB87).
———. 1989, *Ap. J. Suppl.*, **71**, 733 (ATB89).
Allen, D. A., Baines, D. W. T., Blades, J. C., and Whittet, D. C. B. 1982, *M.N.R.A.S.*, **199**, 1017.
Baas, F., Allamandola, L. J., Geballe, T. R., Persson, S. E., and Lacy, J. H. 1983, *Ap. J.*, **265**, 290.
Baas, F., Geballe, T. R., and Walther, D. M. 1986, *Ap. J. (Letters)*, **311**, L97.
Barker, J. R., Allamandola, L. J., and Tielens, A. G. G. M. 1987, *Ap. J. (Letters)*, **315**, L61 (BAT).
Bellamy, L. J. 1966, *The Infrared Spectra of Complex Molecules* (New York: Wiley).
Borghesi, A., Bussoletti, E., and Colangeli, L. 1987, *Ap. J.*, **314**, 422.
Bregman, J. D., Allamandola, L. J., Tielens, A. G. G. M., Geballe, T., and Witteborn, F. C. 1989, *Ap. J.*, **344**, 791.
Bregman, J. D., Campins, H., Witteborn, F. C., Wooden, D. H., Rank, D. M., Allamandola, L. J., Cohen, M., and Tielens, A. G. G. M. 1987, *Astr. Ap.*, **187**, 616.
Butchart, I., McFadzean, A. D., Whittet, D. C. B., Geballe, T. R., and Greenberg, J. M. 1986, *Astr. Ap.*, **154**, L5.
Chlewicki, G., and Laureijs, R. J. 1988, *Astr. Ap.*, **207**, L11.
Cohen, M., Allamandola, L. J., Tielens, A. G. G. M., Bregman, J., Simpson, J. P., Witteborn, F. C., Wooden, D., and Rank, D. 1986, *Ap. J.*, **302**, 737.
Cohen, M., *et al.* 1975, *Ap. J.*, **196**, 179.
Cohen, M., and Kuhi, L. V. 1979, *Ap. J. Suppl.*, **41**, 743.
Cohen, M., Tielens, A. G. G. M., Bregman, J., Witteborn, F. C., Rank, D. M., Allamandola, L. J., Wooden, D. H., and de Muizon, M. 1989, *Ap. J.*, **341**, 246.
Cohen, M., and Witteborn, F. C. 1985, *Ap. J.*, **294**, 345.
Cyvin, S. J., Cyvin, B. N., Brunvoll, J., Whitmer, J. C., and Klaeboe, P. 1982, *Zs. Naturforsch.*, **37A**, 1359.
Cyvin, S. J., and Klaeboe, P. 1988, private communication.
de Muizon, M., Geballe, T. R., d'Hendecourt, L. B., and Baas, F. 1986, *Ap. J. (Letters)*, **306**, L105.
d'Hendecourt, L. B., and Allamandola, L. J. 1986, *Astr. Ap. Suppl.*, **64**, 453.
d'Hendecourt, L. B., and Léger, A. 1987, in *Planetary and Protoplanetary Nebulae: From IRAS to ISO*, ed. A. Preite Martinez (Dordrecht: Reidel), p. 203.
Donn, B. 1988, private communication.
Duley, W. W., and Williams, D. A. 1981, *M.N.R.A.S.*, **196**, 296.
Elias, J. H. 1978, *Ap. J.*, **224**, 857.
Frenklach, M., and Feigelson, E. D. 1989, *Ap. J.*, **341**, 372.
Geballe, T. R., Lacy, J. H., Persson, S. E., McGregor, P. J., and Soifer, B. T. 1985, *Ap. J.*, **292**, 500.
Geballe, T. R., Noll, K. S., Whittet, D. C. B., and Waters, L. B. F. M. 1989*a*, *Ap. J. (Letters)*, **340**, L29.
Geballe, T. R., Tielens, A. G. G. M., Allamandola, L. J., Moorhouse, A., and Brand, P. W. J. L. 1989*b*, *Ap. J.*, **341**, 278.
Gillett, F. C., Forrest, W. J., Merrill, K. M., Capps, R. W., and Soifer, B. T. 1975, *Ap. J.*, **200**, 609.
Glass, I. S. 1979, *M.N.R.A.S.*, **187**, 305.
Grasdalen, G., Joyce, R., Knacke, R. F., Strom, S. E., and Strom, K. M. 1975, *A.J.*, **80**, 117.
Herbig, G. H. 1960, *Ap. J. Suppl.*, **4**, 337.
Herzberg, G. 1945, *Molecular Spectra and Molecular Structure II. Infrared and Raman Spectra of Polyatomic Molecules* (London: van Nostrand).
Leinert, Ch., and Haas, M. 1989, *Astr. Ap.*, **221**, 110.
Léger, A., and d'Hendecourt, L. 1987, in *Polycyclic Aromatic Hydrocarbons and Astrophysics*, ed. L. Léger, L. d'Hendecourt, and N. Boccara (Dordrecht: Reidel), p. 223.
Léger, A., d'Hendecourt, L., and Défourneau, D. 1989, *Astr. Ap.*, **216**, 148.
Léger, A., and Puget, J. L. 1984, *Astr. Ap.*, **137**, L5.
Mortera, C., and Low, M. J. D. 1983, *Carbon*, **2**, 283.
Piseri, L., and Zerbi, G. 1968, *J. Chem. Phys.*, **48**, 3561.
Reddy, K. V., Heller, D. F., and Berny, M. J. 1982, *J. Chem. Phys.*, **76**, 2814.
Roche, P. F., Allen, D. A., and Bailey, J. A. 1986, *M.N.R.A.S.*, **220**, 7P.
Salisbury, D. W., Allen J. E., Jr., Donn, B., Khanna, R. K., and Moore, W. J. 1988, in *Experiments on Cosmic Dust Analogues*, ed. E. Bussoletti *et al.* (Dordrecht: Kluwer), p. 129.
Sandford, S. A., and Walker, A. M. 1985, *Ap. J.*, **291**, 838.
Schutte, W. A., Tielens, A. G. G. M., and Allamandola, L. J. 1990, in preparation.
Socrates, G. 1980, *IR Characteristic Group Frequencies* (New York: Wiley).
Thé, P. S., Wesselius, P. R., Tjin A Djie, H. R. E., and Steenman, H. 1986, *Astr. Ap.*, **155**, 347.
Tielens, A. G. G. M., Allamandola, L. J., Barker, J. R., and Cohen, M. 1987, in *Polycyclic Aromatic Hydrocarbons and Astrophysics*, ed. A. Léger, L. d'Hendecourt, and N. Boccara (Reidel: Dordrecht), p. 273 (TABC).
Tokunaga, A. T. 1988, private communication.
Tokunaga, A. T., Nagata, T., Sellgren, K., Smith, R. G., Onaka, T., Nakada, Y., Sakata, A., and Wada, S. 1988, *Ap. J.*, **328**, 709.
van der Zwet, G. P., Allamandola, L. J., , Baas, F., and Greenberg, J. M. 1985, *Astr. Ap.*, **145**, 262.
Wexler, A. S. 1967, *Appl. Spec. Rev.*, **1**, 29.
Whittet, D. C. B., Bode, M. F., Longmore, A. J., Adamson, A. J., McFadzean, A. D., Aitken, D. K., and Roche, P. F. 1988, *M.N.R.A.S.*, **233**, 321.
Whittet, D. C. B., McFadzean, A. D., and Geballe, T. R. 1984, *M.N.R.A.S.*, **211**, 29P.
Whittet, D. C. B., and van Breda, I. G. 1980, *M.N.R.A.S.*, **192**, 467.
Whittet, D. C. B., Williams, P. M., Bode, M. F., Davies, J. K., and Zealey, W. J. 1983, *Astr. Ap.*, **123**, 301.
Wilson, E. B., Decius, J. C., and Cross, P. C. 1955, *Molecular Vibrations* (New York: McGraw Hill), p. 247.
Witteborn, F. C., and Bregman, J. D. 1984, *Cryogenic Optical Systems and Instruments*, ed. R. K. Melugin (*Proc. SPIE*, Vol. **509**), p. 123.
Witteborn, F. C., Sandford, S. A., Bregman, J. D., Allamandola, L. J., Cohen, M., Wooden, D. H., and Graps, A. L. 1989, *Ap. J.*, **341**, 270.

L. J. Allamandola, M. Cohen, W. A. Schutte, and D. H. Wooden: Mailstop 245-6, NASA/Ames Research Center, Moffett Field, CA 94035

A. G. G. M. Tielens: Mailstop 245-3, NASA/Ames Research Center, Moffett Field, CA 94035